Korean J. Chem. Eng., **28**(1), 149-155 (2011)
DOI: 10.1007/s11814-010-0342-0

Removal of methylene blue dye from aqueous solution by activated carbon prepared from cashew nut shell as a new low-cost adsorbent

Ponnusamy Senthil Kumar*,†, Subramaniam Ramalingam, and Kannaiyan Sathishkumar***

*Department of Chemical Engineering, SSN College of Engineering, Chennai 603 110, India
**Chemical and Biomolecular Engineering Department, Tulane University, New Orleans, LA 70118-5674, U.S.A.
(*Received 26 November 2009 • accepted 2 June 2010*)

Abstract−Methylene blue dye was adsorbed on an adsorbent prepared from cashew nut shell. A batch adsorption study was carried out with variable adsorbent amount, initial dye concentration, contact time and pH. Studies showed that the pH of aqueous solutions affected dye removal as a result of removal efficiency increased with increasing solution pH. The experimental data were analyzed by the Langmuir, Freundlich, Redlich-Peterson, Koble-Corrigan, Toth, Temkin, Sips and Dubinin-Radushkevich models of adsorption using MATLAB 7.1. The experimental data yielded excellent fits within the following isotherm order: Redlich-Peterson>Toth>Sips>Koble-Corrigan>Langmuir>Temkin>Dubinin-Radushkevich>Freundlich, based on its correlation coefficient values. Three simplified kinetic models including a pseudo-first-order, pseudo-second-order and intraparticle diffusion equations were selected to follow the adsorption process. It was shown that the adsorption of methylene blue could be described by the pseudo-second-order equation. The results indicate that cashew nut shell activated carbon could be employed as a low cost alternative to commercial activated carbon in the removal of dyes from wastewater.

Key words: Cashew Nut Shell, Activated Carbon, Methylene Blue, Adsorption, Isotherms, Kinetics

INTRODUCTION

Methylene blue (MB), a basic dye, was used initially for dyeing of silk, leather, plastics, paper, and cotton mordant with tannin, as well as for the production of ink and copying paper in the office supplies industry. The discharge of these dyes in the environment is worrying for both toxicological and aesthetical reasons as dyes impede light penetration, damage the quality of the receiving streams and are toxic to food chain organisms [1]. Since dyes have a synthetic origin and complex aromatic molecular structures, they are inert and difficult to biodegrade when discharged into waste streams. This aspect has always been overlooked in their discharge [2]. The removal of synthetic dyes is of great concern, since some dyes and their degradation products may be carcinogens and toxic and, consequently, their treatment cannot depend on biodegradation alone [3,4].

The most commonly used methods for color removal are biological and chemical precipitation. However, these processes are effective and economic only in cases where solute concentrations are relatively high [5]. There are advantages and disadvantages of various methods of dye removal from wastewaters [6]. Many physicochemical methods have been tested, but only that of adsorption is considered to be superior to other techniques. This is attributed to its low cost, easy availability, simplicity of design, high efficiency, easy operation, biodegradability and ability to treat dyes in more concentrated forms [7,8]. Activated carbon adsorption is one such method which has a great potential for the removal of dyes from wastewater [9-14]. Commercially available activated carbons are usually derived from natural materials such as wood or coal and still considered expensive [15]. This has led to the search for cheaper substitutes. Hence, low-cost activated carbons based on agricultural solid wastes have been investigated for a long time. Agricultural byproducts and waste materials used for the production of activated carbons include plum kernels [16], cassava peel [17], bagasse [18], jute fiber [19], palm-tree cobs [20], rice husks [21], olive stones [22], date pits [23], fruit stones and nutshells [24], rattan sawdust [25], peach stones [26], oil palm shell [27], orange peel carbon [28] and Egyptian rice hull [29]. The present investigation reports the results of removal of methylene blue dye from aqueous solution by adsorption onto activated carbon prepared from low cost cashew nut shell (CNS). The objective of the present work is to examine the effectiveness of the prepared activated carbon in removing MB from aqueous solution. The kinetic data and equilibrium data of adsorption studies were processed to understand the adsorption mechanism of the dye molecules onto the cashew nut shell activated carbon (CNSAC).

EXPERIMENTAL

1. Preparation and Characterization of CNSAC

The CNS was collected from Pudukkottai District, Tamilnadu, India. It was washed with hot distilled water to remove dust like impurities, dried and the material was finally sieved to discrete sizes. The raw material was then carbonized at 700 °C under nitrogen atmosphere for 1 h. A certain amount of produced char then was soaked with potassium hydroxide (KOH) at impregnation ratio of 1 : 1. The mixture was dehydrated in an oven overnight at 105±1 °C and then pyrolyzed in a stainless steel vertical tubular reactor placed in a tube furnace under high-purity nitrogen (99.99%) flow of 150 cm^3/min

†To whom correspondence should be addressed.
E-mail: senthilkumarp@ssn.edu.in, senthilchem8582@gmail.com

to a final temperature of 850 ºC and 2 h soaking. Once the final temperature was reached, the nitrogen gas flow was switched to carbon dioxide and activation was continued for 2 h. The activated product was then cooled to room temperature and washed with deionized water to remove remaining chemical. Subsequently the sample was transferred to a beaker containing 250 mL solution of HCl (about 0.1 mol/L) stirred for 1 h, and then washed with hot deionized water. The textual characterization of the CNSAC was carried out by N_2 adsorption at 77 K using Autosorb I, supplied by Quantachrome Corporation, USA. The Brunauere EmmetteTeller (BET) (N_2, 77 K) is the most usual standard procedure used when characterizing an activated carbon [30]. It was found that the BET surface area, average pore diameter and pore volume of the CNSAC were 984 m^2/g, 2.52 nm and 0.552 cm^3/g, respectively.

FT-IR spectroscopy is an important analytical technique that detects the vibration characteristics of chemical functional groups present on adsorbent surfaces. Besides porosity, adsorption behavior of CNSAC is also influenced by the chemical reactivity of the surface especially in the form of chemisorbed oxygen in various forms of functional groups. The CNSAC spectrum shows the surface functional group with the following peaks: a peak at 3,432 cm^{-1}: -OH group of phenol; 2,921 cm^{-1}: methylene group (-CH_2-); 2,844 cm^{-1}: -O-CH_3 or two bands for aldehyde group; 2,160 cm^{-1}: acetals; 1,565 cm^{-1}: carbonyl group in quinone as well as γ-pyrone structure; 1,443 cm^{-1} and 1,110 cm^{-1}: ketones, alcohols, pyrones and aromatic C-H in-plane deformations. The formation of stronger peaks for pyrone-type structures, ether, carbonyl groups employed a basic character of CNSAC. These basic sites in the form of unsaturated bonds between adjacent C-atoms or even non-oxygenated sites with electron donating properties would act as Lewis basic centers that accept protons from aqueous solutions.

2. Adsorbate

Methylene blue supplied by Merck-India was used as an adsorbate and was not purified prior to use. A stock solution of MB dye was prepared (500 mg/L) by dissolving the required amount of dye powder in double distilled water. The stock solution was diluted with double distilled water to obtain desired concentration ranging from 50 to 250 mg/L. MB has a molecular weight of 373.9 g/mol, which corresponds to methylene blue hydrochloride with three groups of water. Before mixing the adsorbent, the pH of the solution was adjusted to the required value with 0.1 M NaOH or 0.1 M HCl.

3. Analysis

The concentration of MB in the supernatant solution before and after adsorption was determined using a double beam UV-vis spectrophotometer (Shimadzu, Japan) at 668 nm. The supernatant from the CNSAC did not exhibit any absorbance at this wavelength and also the calibration curve was very much reproducible and linear over the concentration range used in this work. The pH of solution was measured with a Hanna pH meter using a combined glass electrode (Model HI 9025C, Singapore).

4. Adsorption Experiment

Batch studies were carried out at 30 ºC. In the adsorption experiment, the weighed quantity of CNSAC was taken in an Erlenmeyer flask (250 mL) containing 100 mL wastewater sample. The pH of the solution was adjusted to the desired value by adding 0.1 M NaOH or HCl and the solution-CNSAC mixture was shaken for a predetermined period using a wrist action shaker operated at 120 rpm. Kinetics of adsorption was determined by analyzing adsorptive uptake of the dye at different time intervals. Independent bottles containing 100 mL wastewater sample and 0.2 g CNSAC were used during the kinetic studies to get accurate results for each point on the graph. Isothermal studies were conducted with different initial concentrations (50-250 mg/L) and 100 mL sample by shaking the reaction mixture for equilibrium time. The residual dye concentration in the reaction mixture was analyzed by centrifuging the reaction mixture and then measuring the absorbance of the supernatant at the wavelength that correspond to the maximum absorbance of the sample. Dye concentration in the reaction mixture was calculated from the calibration curve. The λ_{max} values of the wastewater samples varied ±10 nm from the λ_{max} values of pure dyes at a fixed pH. The amount of dye adsorbed onto the CNSAC, q_e (mg/g), was calculated by the following mass balance relationship:

$$q_e = \frac{(C_i - C_e)V}{W} \quad (1)$$

where C_o and C_e are the initial and equilibrium liquid-phase concentrations of dye, respectively (mg/L), V the volume of the solution (L), and W is the mass of the CNSAC used (g).

RESULTS AND DISCUSSION

1. Effect of pH

Effect of pH on adsorption was studied using 50 mg/L dye concentration, pH 2-10 at 30 ºC as given in Fig. 1. The dye adsorption was significantly changed over the pH value of 2-8. The dye adsorption was constant at pH 9-10. The lowest dye adsorption was recorded at pH 2 (7.72 mg/g). The equilibrium adsorption (q_e) was found to increase with increasing pH. The q_e increases from 7.72 to 24.51 mg/g for an increase in pH from 2 to 10. Lower adsorption of MB at acidic pH is probably due to the presence of excess H^+ ions competing with the cation groups on the dye for adsorption sites. At higher pH, the surface of CNSAC particles may get negatively charged, which enhances the positively charged dye cations through electrostatic forces of attraction [31,32].

2. Effect of Adsorbent Dose

Fig. 2 shows the plot between amounts of dye adsorbed q_e against adsorbent concentration (g/L). From the figure it was observed that

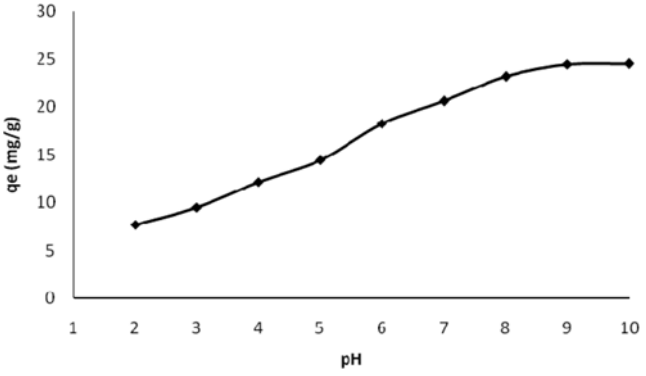

Fig. 1. Effect of pH on MB removal (MB concentration=50 mg/L, adsorbent dose=2 g/L, volume of sample=100 mL and equilibrium time=90 min).

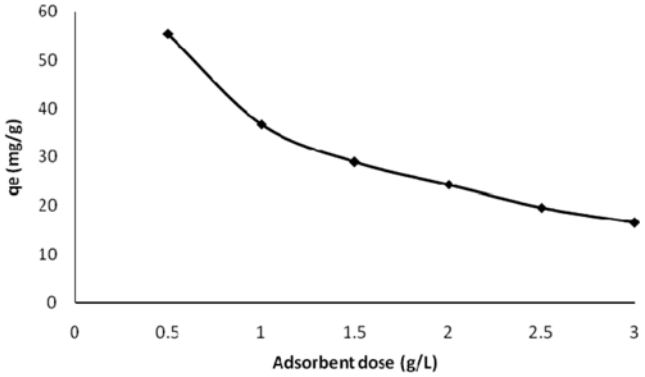

Fig. 2. Effect of adsorbent dose on MB removal (MB concentration =50 mg/L, volume of sample=100 mL and equilibrium time =90 min).

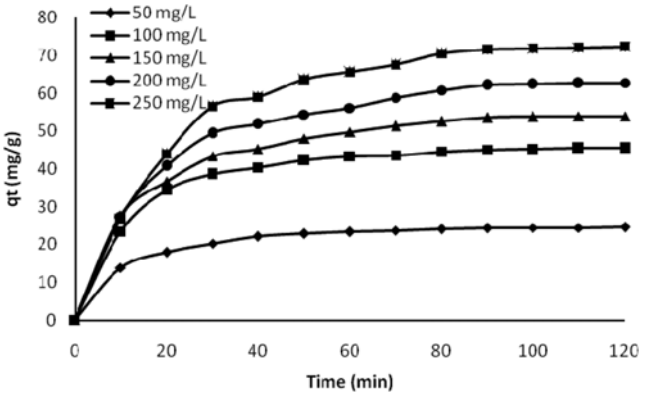

Fig. 4. Effect of contact time (MB concentrations=50-250 mg/L, adsorbent dose=2 g/L, volume of sample=100 mL and contact time=0-120 min).

the amount of dye adsorbed varied with varying adsorbent dose and it decreased with increase in adsorbent dose. The amount of dye adsorbed decreased from 55.48 to 16.53 mg/g for an increase in adsorbent dose from 0.5 to 3 g/L, whereas the percent dye removal increased from 55.48 to 99.17% with an increase in adsorbent dose 0.5 to 3 g/L (not shown). At higher adsorbent dose to solute concentration ratio, there is very fast superficial sorption onto the adsorbent surface that produces a lower solute concentration in solute than when adsorbent to solute concentration ratio is lower. This is because a fixed amount of adsorbent can only adsorb a certain amount of dye. Therefore, the more adsorbent the dosage, the larger is the volume of effluent that a fixed dose of adsorbent can purify. The decrease in amount of dye adsorbed q_e (mg/g) with increasing adsorbent dose is due to the split in the flux or the concentration gradient between solute concentration in the solution and the solute concentration in the surface of the adsorbent. Thus, with increasing adsorbent dose, the amount of dye adsorbed onto unit weight of adsorbent gets splitted thus causing a decrease in q_e value with increasing adsorbent dose concentration.

3. Effect of Initial Dye Concentration

Fig. 3. shows the plot between the amount of dye adsorbed q_e versus initial dye concentration. It is evident from the figure that the amount of dye adsorbed gets increased from 24.48 to 72.36 mg/g for an increase in initial dye concentration from 50 to 250 mg/L, whereas the percent dye removal decreases from 89.91 to 60.89% (not shown) for an increase in initial dye concentration from 50 to 250 mg/L. At low dye concentrations the ratio of surface active sites to the total dye molecules in the solution is high and hence all dye molecules may interact with the CNSAC and be removed from the solution. However, the amount of dye adsorbed per unit weight of adsorbent, q_e, is higher at high concentrations as shown in the figure.

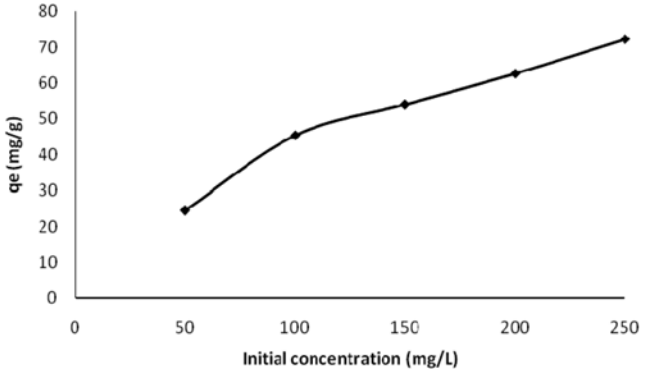

Fig. 3. Effect of initial dye concentration (MB concentrations=50-250 mg/L, adsorbent dose=2 g/L, volume of sample=100 mL and equilibrium time=90 min).

4. Effect of Contact Time

The relation between adsorption of MB and contact time was investigated to identify the rate of dye removal. Fig. 4. shows the dye uptake on adsorbent (q_t) at different initial dye concentrations ranging from 50-250 mg/L. The adsorption increases with the increasing contact time and it was found that the rapid adsorption of dye in the first 60 min and thereafter the adsorption rate decreased gradually and the adsorption reached equilibrium in about 90 min. Increase in contact time up to 120 min showed that the MB removal by CNSAC was only by about 0.8% over those obtained for 90 min contact time. Aggregation of dye molecules with the increase in contact time makes it almost impossible to diffuse deeper into the adsorbent structure at highest energy sites. This aggregation negates the influence of contact time as the micropores get filled up and start offering resistance to diffusion of aggregated dye molecules in the adsorbents. This is the reason why an insignificant enhancement in adsorption is effected in 120 min as compared to that in 90 min. Since the difference in the adsorption values at 90 min and at 120 min is very small, after 90 min contact, a steady-state approximation was assumed and a quasi-equilibrium situation was accepted. Further experiments were conducted for 90 min contact time only. The adsorption curves were single, smooth and continuous leading to saturation and indicated the possible mono-layer coverage on the surface of adsorbents by the dye molecules [9,33].

5. Adsorption Equilibrium Study

The adsorption isotherm indicates how the adsorption molecules distribute between the liquid phase and the solid phase when the adsorption process reaches an equilibrium state. The analysis of the isotherm data by fitting them to different isotherm models is an important step to find the suitable model that can be used for design purpose. To adapt for the considered system, an adequate model that can reproduce the experimental results obtained, equations of

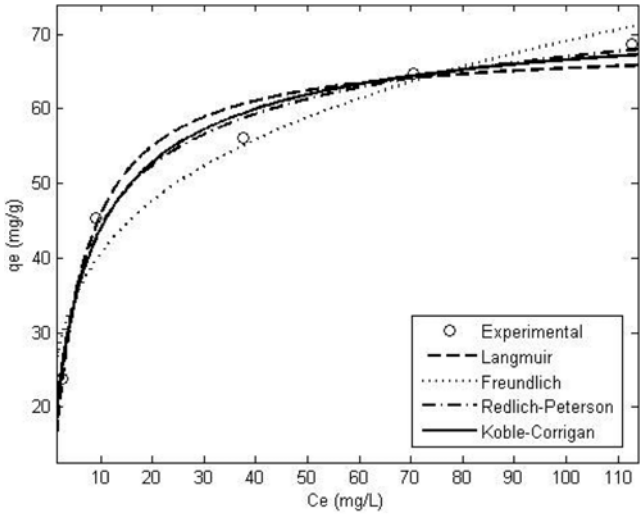

(a)

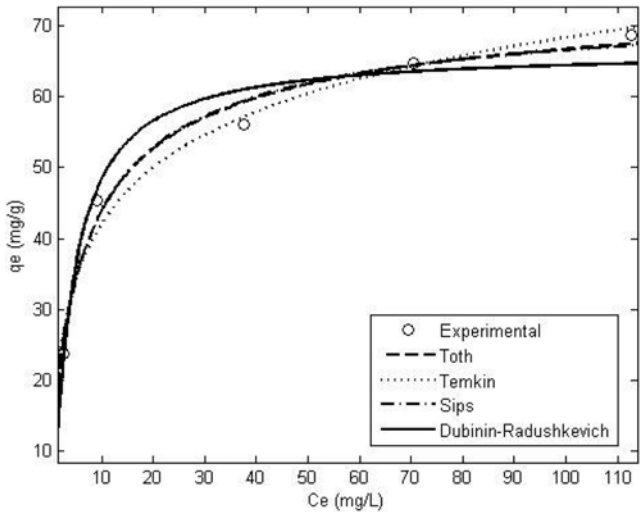

(b)

Fig. 5. (a) Adsorption isotherm (MB concentrations=50-250 mg/L, adsorbent dose=2 g/L, volume of sample=100 mL and equilibrium time=90 min). (b) Adsorption isotherm (MB concentrations=50-250 mg/L, adsorbent dose=2 g/L, volume of sample=100 mL and equilibrium time=90 min).

Langmuir [34], Freundlich [35], Redlich-Peterson [36], Koble-Corrigan [37], Toth [38], Temkin [39], Sips [40] and Dubinin-Radushkevich [41] have been considered.

The experimental data on the effect of an initial concentration of MB on the CNSAC of the test medium were fitted to the isotherm models using MATLAB 7.1 and the graphical representations of these models are presented in Fig. 5(a) and (b). All of the constants are presented in Table 1. The value of R^2 nearer to 1 indicates that the respective equation better fits the experimental data. The representations of the experimental data by all models equation result in a non-linear curve with R^2 values of a least 0.943 as tabulated in Table 1. The experimental data yielded excellent fits with in the following isotherms order: Redlich-Peterson>Toth>Sips>KobleCorrigan >Langmuir>Temkin>DubininRadushkevich>Freundlich, based on its R^2 values. The plotted equations obtained from the graph are presented in Table 1. It was found that the Redlich-Peterson best represents the equilibrium adsorption of MB on CNSAC. The correlation coefficients for Redlich-Peterson isotherm are highest in comparison to the values obtained for the Langmuir, Freundlich, Koble-Corrigan, Toth, Temkin, Sips and Dubinin-Radushkevich isotherms. Therefore, Redlich-Peterson is the best-fit isotherm equation for the adsorption of MB on CNSAC. The comparison of maximum monolayer adsorption capacity of some dyes onto various adsorbents is presented in Table 2. It shows that the CNSAC studied in this work has very large adsorption capacity. This is due to its high surface area (984 m^2/g).

Table 1. The value of parameters for each isotherm models used in the studies

Isotherm model	Parameter	R^2	Equation
Langmuir	q_m=68.72 K_L=0.201	0.981	$q_e=\frac{13.813C_e}{1+0.201C_e}$
Freundlich	K_F=23.82 n=4.325	0.943	$q_e=23.82C_e^{0.231}$
Redlich-Peterson	K_R=19.24 α_R=0.408 β=0.916	0.989	$q_e=\frac{19.24C_e}{1+0.408C_e^{0.916}}$
Koble-Corrigan model	a=18.51 b=0.248 n=0.759	0.983	$q_e=\frac{18.51C_e^{0.759}}{1+0.248C_e^{0.759}}$
Toth	f=77.23 g=1.972 d=0.649	0.985	$q_e=\frac{77.23C_e}{[1.972+(C_e)^{0.649}]^{1.541}}$
Temkin	A=3.948 B=4.963	0.978	$q_e=4.963\ln(3.948C_e)$
Sips	Q_{max}=74.71 K_S=0.248 n=1.317	0.983	$q_e=\frac{18.528C_e^{0.759}}{1+0.248C_e^{0.759}}$
Dubinin-Radushkevich	q_m=66.62 $\beta=6.15\times10^{-8}$ E=2849.014	0.964	$q_e=66.626e^{-6.15\times10^{-8}\varepsilon^2}$

Table 2. Comparison of maximum monolayer adsorption of some dyes onto various adsorbents

Dyes	Adsorbents	q_m (mg/g)	Reference
Methylene blue	Rattan-AC	294.12	[25]
Methylene blue	Jute fiber carbon	225.64	[19]
Methylene blue	CNS-AC	**68.72**	**This work**
Methylene blue	Hazelnut shell-AC	8.82	[24]
Methylene blue	Apricot stones-AC	4.11	[24]
Methylene blue	Walnut shell-AC	3.53	[24]
Methylene blue	Almond shell-AC	1.33	[24]

6. Adsorption Kinetics

To examine the controlling mechanism of adsorption processes such as mass transfer and chemical reaction, pseudo-first-order, pseudo-second-order and intraparticle diffusion kinetic equations were used to test the experimental data. The pseudo-first-order kinetic model was suggested by Lagergren [42] for the adsorption of solid/liquid systems and its formula is given as:

$$\frac{dq_t}{dt} = k_{ad}(q_e - q_t) \quad (2)$$

After integration by applying the initial conditions q_t=0 at t=0 and q_t=q_t at t=t, Eq.(2) becomes:

$$\log\left(\frac{q_e}{q_e - q_t}\right) = \frac{k_{ad}}{2.303}t \quad (3)$$

Eq. (3) can be rearranged to obtain a linear form:

$$\log(q_e - q_t) = \log q_e \frac{k_{ad}}{2.303}t \quad (4)$$

where q_t is the adsorption capacity at time t (mg/g) and k_{ad} (min^{-1}) is the rate constant of the pseudo-first-order adsorption, was applied to the present study of dye adsorption. The rate constant, k_{ad} and correlation coefficients of the dye under different concentrations were calculated from the linear plots of $\log(q_e - q_t)$ versus t (Fig. 6) and listed in Table 3. The correlation coefficients for the pseudo-first-order kinetic model are low. Moreover, a large difference of equilibrium adsorption capacity (q_e) between the experiment and calculation was observed, indicating a poor pseudo-first-order fit to the experimental data.

The kinetic data were further analyzed using Ho's pseudo-second-order kinetics model. This model is based on the assumption the sorption follows second-order chemisorption. It can be expressed as [43]:

$$\frac{dq_t}{dt} = k(q_e - q_t)^2 \quad (5)$$

Integrating Eq. (5) and applying the boundary conditions, gives:

$$\left(\frac{1}{q_e - q_t}\right) = \frac{1}{q_e} + kt \quad (6)$$

Eq. (6) can be rearranged to obtain a linear form:

$$\frac{t}{q_t} = \frac{1}{h} + \frac{1}{q_e}t \quad (7)$$

where $h=kq_e^2$ (mg $g^{-1}min^{-1}$) can be regarded as the initial adsorption rate as $t \rightarrow 0$ and k is the rate constant of pseudo-second-order adsorption (g $mg^{-1}min^{-1}$). The plot t/q_t versus t (Fig. 7) should give a straight line if pseudo-second-order kinetics is applicable and q_e, k and h can be determined from the slope and intercept of the plot, respectively. At all studied initial dye concentrations, straight lines with extremely high correlation coefficients (>0.996) were obtained. In addition, the calculated q_e values also agree with the experimental data in the case of pseudo-second-order kinetics. These suggest that the adsorption data are well represented by pseudo-second-order kinetics and the rate-limiting step of MB onto CNSAC may be chemisorption. From Table 3, the values of the rate constant k decrease with increasing initial dye concentration for the CNSAC. The reason for this behavior can be attributed to the lower competition for the sorption surface sites at lower concentration. At higher concen-

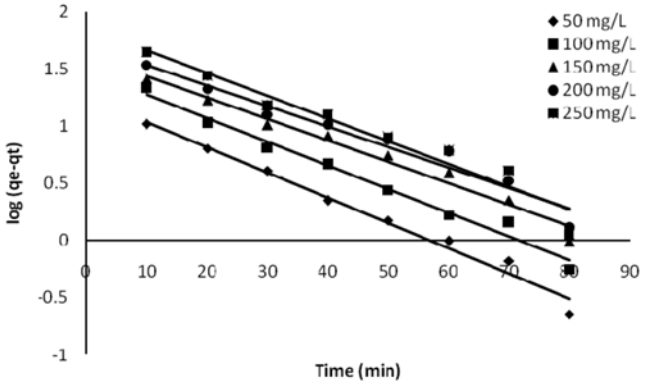

Fig. 6. Pseudo-first-order reaction for MB adsorbed onto CNSAC at different concentrations (MB concentrations=50-250 mg/L, adsorbent dose=2 g/L, volume of sample=100 mL and equilibrium time=90 min).

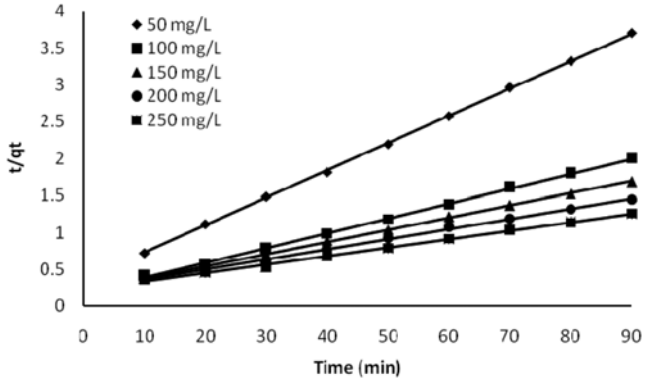

Fig. 7. Pseudo-second-order reaction for MB adsorbed onto CNSAC at different concentrations (MB concentrations=50-250 mg/L, adsorbent dose=2 g/L, volume of sample=100 mL and equilibrium time=90 min).

Table 3. Comparison between the adsorption rate constants, q_e, estimated and correlation coefficients associated with pseudo-first-order and to the pseudo-second-order rate equations and intraparticle diffusion

Initial MB concn. (mg/L)	Pseudo-first-order rate equation			Pseudo-second-order rate equations				Intraparticle diffusion			
	k_{ad} (min^{-1})	q_e (mg/g)	R^2	k (g mg^{-1} min^{-1})×10^{-3}	q_e, cal (mg/g)	h (mg g^{-1} min^{-1})	q_e,exp (mg/g)	R^2	k_p (mg/g·$min^{1/2}$)	C	R^2
50	0.051	18.323	0.983	3.845	27.027	2.809	24.28	0.999	1.567	10.69	0.900
100	0.046	30.619	0.984	2.094	49.485	5.128	45.075	0.999	3.188	17.23	0.907
150	0.041	42.364	0.975	1.497	56.271	4.739	53.265	0.999	3.893	18.90	0.938
200	0.041	52.481	0.958	1.105	64.285	4.566	62.11	0.998	5.037	17.09	0.921
250	0.044	64.863	0.947	0.798	74.135	4.386	71.65	0.997	6.549	13.89	0.908

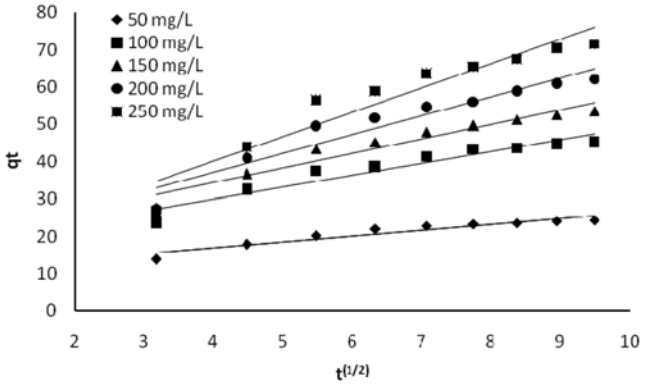

Fig. 8. Intraparticle diffusion (MB concentrations=50-250 mg/L, adsorbent dose=2 g/L, volume of sample=100 mL and equilibrium time=90 min).

trations, the competition for the surface active sites will be high and consequently lower sorption rates are obtained.

To gain insight into the mechanisms and rate controlling steps affecting the kinetics of adsorption, the kinetic experimental results were fitted to Weber's intraparticle diffusion [44]. The kinetic results were analyzed by the intraparticle model to elucidate the diffusion mechanism, which model is expressed as:

$$q_t = k_p t^{1/2} + C \quad (8)$$

where C is the intercept and k_p is the intraparticle diffusion rate constant, ($mg/gmin^{1/2}$), which can be evaluated from the slope of the linear plot of q_t versus $t^{(1/2)}$ [44] as shown in Fig. 8. The intercept of the plot reflects the boundary layer effect. The larger the intercept, the greater the contribution of the surface sorption in the rate-controlling step. The calculated intraparticle diffusion coefficient k_p values are listed in Table 3. If the regression of q_t versus $t^{(1/2)}$ is linear and passes through the origin, then intraparticle diffusion is the sole rate-limiting step. However, the linear plots at each concentration did not pass through the origin, which indicates that the intraparticle diffusion was not only rate controlling step.

CONCLUSION

Kinetic and equilibrium studies were reported for the adsorption of MB from aqueous solutions onto activated carbon prepared from cashew nut shell which can be effectively used as an adsorbent for the removal of dye. Since CNS used in this work is freely, abundantly and locally available, the resulting adsorbent is expected to be economically viable for removal of MB from aqueous solution. Experimental data indicate that the adsorption capacity was dependent of operating variables such as pH, adsorbent quantity, contact time and initial dye concentration. The adsorption process was strongly pH-dependent. The equilibrium data have been analyzed using Langmuir, Freundlich, Redlich-Peterson, Koble-Corrigan, Toth, Temkin, Sips and Dubinin-Radushkevich isotherms. The characteristic parameters for each isotherm and related correlation coefficients have been determined. The suitability of the pseudo-first- and second-order equations and intraparticle diffusion kinetic model for the sorption of MB onto CNSAC is also discussed. The pseudo-second-order kinetic model agrees very well with the dynamical behavior for the adsorption of MB onto CNSAC for different initial MB concentrations over the whole range studied. The CNSAC appeared to be suitable for the removal of MB from aqueous solutions.

REFERENCES

1. T. V. N. Padmesh, K. Vijayaraghavan, G. Sekaran and M. Velan, *Dyes Pigm.*, **71**, 77 (2006).
2. Y. S. Ho, T. H. Chiang and Y. M. Hsueh, *Process Biochem.*, **40**, 119 (2005).
3. A. Reife, Dyes, Environmental Chemistry, Kirk-Othmer Encyclopedia of Chemical Technology, 4th Ed. Washington, John Wiley & Sons, 753 (1993).
4. U. Pagga and D. Braun, *Chemosphere*, **15**, 479 (1986).
5. V. Vadivelan and K. V. Kumar, *J. Colloid Interf. Sci.*, **286**, 90 (2005).
6. V. K. Garg, M. Amita, R. Kumar and R. Gupta, *Dyes Pigm.*, **63**, 243 (2004).
7. R. Sanghi and B. Bhattacharya, *Color Technol.*, **118**, 256 (2002).
8. V. Meshko, L. Markovska, M. Mincheva and A. E. Rodrigues, *Water Res.*, **35**, 3357 (2001).
9. P. K. Malik, *Dyes Pigm.*, **56**, 239 (2003).
10. M. Goyal, S. Singh and R. C. Bansal, *Carbon Science*, **5**, 170 (2004).
11. F. K. Bangash and A. Manaf, *J. Chem. Soc. Pak.*, **26**, 111 (2004).
12. E. Lorenc-Grabowska and G. Gryglewicz, *Dyes Pigm.*, **68**, 1 (2006).
13. C. Namasivayam and D. Kavitha, *Dyes Pigm.*, **54**, 47 (2002).
14. R. L. Teng, F. Ch. Wu and R. S. Juang, *Carbon*, **41**, 487 (2003).
15. B. K. Singh and N. S. Rawat, *J. Chem. Technol. Biotechnol.*, **61**, 307 (1994).
16. F. C. Wu, R. L. Tseng and R. S. Juang, *J. Hazard. Mater.*, **B69**, 287 (1999).
17. S. Rajeshwarisivaraj, P. Senthilkumar and V. Subburam, *Bioresour. Technol.*, **80**, 233 (2001).
18. W. T. Tsai, C. Y. Chang, M. C. Lin, S. F. Chien, H. F. Sun and M. F. Hsieh, *Chemosphere*, **45**, 51 (2001).
19. S. Senthilkumaar, P. R. Varadarajan, K. Porkodi and C. V. Subbhuraam, *J. Colloid Interf. Sci.*, **284**, 78 (2005).
20. J. Avom, J. K. Mbadcam, C. Noubactep and P. Germain, *Carbon*, **35**, 365 (1997).
21. N. Yalcin and V. Sevinc, *Carbon*, **38**, 1943 (2000).
22. A. H. El-Sheikh and A. P. Newman, *J. Anal. Appl. Pyrol.*, **71**, 151 (2004).
23. B. S. Girgis and A. A. El-Hendawy, *Micropor. Mesopor. Mater.*, **52**, 105 (2002).
24. A. Aygun, S. Yenisoy-Karakas and I. Duman, *Micropor. Mesopor. Mater.*, **66**, 189 (2003).
25. B. H. Hameed, A. L. Ahmad and K. N. A. Latiff, *Dyes Pigm.*, **75**, 143 (2007).
26. A. A. Attia, B. S. Girgis and N. A. Fathy, *Dyes Pigm.*, **76**, 282 (2008).
27. I. A. W. Tan, A. L. Ahmad and B. H. Hameed, *Desalination*, **225**, 13 (2008).
28. A. Khaled, A. El. Nemr, A. El-Sikaily and O. Abdelwahab, *Desalination*, **238**, 210 (2009).
29. M. M. El-Halwany, *Desalination*, **250**, 208 (2010).
30. K. S. W. Sing, D. H. Everett, R. A. W. Haul, L. Moscou, R. A. Pierotti and J. Rouquerol, *Pure Appl. Chem.*, **57**, 603 (1985).
31. S. Wang, L. Li, H. Wu and Z. H. Zhu, *J. Colloid Interf. Sci.*, **292**, 336 (2005).

32. B. H. Hameed, D. K. Mahmoud and A. L. Ahmed, *J. Hazard. Mater*., **158**, 65 (2008).
33. Y. Wong and J. Yu, *Water Res*., **33**, 3512 (1999).
34. I. Langmuir, *J. Amer. Chem. Soc*., **40**, 1361 (1918).
35. H. M. F. Freundlich, *J. Phys. Chem*., **57**, 385 (1906).
36. O. Redlich and D. L. Peterson, *J. Phys. Chem*., **63**, 1024 (1959).
37. R. A. Koble and T. E. Corrigan, *Ind. Eng. Chem*., **44**, 383 (1952).
38. J. Toth, *Acta Chim. Acad. Sci. Hung*., **69**, 311 (1961).
39. M. J. Temkin and V. Pyzhev, *Acta Physicochim. URSS*, **12**, 217 (1940).
40. B. Volesky, *Hydrometallurgy*, **71**, 179 (2003).
41. M. M. Dubinin and L. V. Radushkevich, *Chem. Zentr*., **1**, 875 (1947).
42. S. Lagregren, *Kungl. Sven. Veten. Akad. Handl*., **24**, 1 (1898).
43. Y. S. Ho and G. McKay, *Process Biochem*., **34**, 451 (1999).
44. W. J. Weber and Jr. J. C. Morriss, *J. Sanit. Eng. Div. Proc. Am. Soc. Civ. Eng*., **89**, 31 (1963).